

## 16. $\beta$ -Helical Structures of Boc-(L-Val-D-Val)<sub>6</sub>-OMe in the Crystalline State and in Chloroform<sup>1)</sup>

by Gian Paolo Lorenzi, Hans Jäckle and Lera Tomasic

Technisch-Chemisches Laboratorium, ETH-Zentrum, CH-8092 Zürich

and Carlo Pedone and Benedetto Di Blasio

Istituto Chimico, Università di Napoli, I-80134 Napoli

(9. VIII. 82)

---

### Summary

A conformational study was carried out on Boc-(L-Val-D-Val)<sub>6</sub>-OMe in the crystalline state by X-ray and IR, and by <sup>1</sup>H-NMR, in chloroform. The dodecapeptide crystallizes from CHCl<sub>3</sub>/EtOAc with a left-handed helical structure of the type  $\uparrow\beta^{5,6}$ , and from CHCl<sub>3</sub>/MeOH (or MeOH) with a different structure. In chloroform it forms three slowly interconverting species: one is a  $\uparrow\beta^{5,6}$  left-handed helical species, and the other two are most likely single-stranded  $\beta^{4,4}$  helical species of opposite handedness. The double-stranded helical species is predominant in fresh solutions of samples obtained from CHCl<sub>3</sub>/EtOAc. Because of the slow conversion or formation of this species some hours are needed to reach the conformational equilibrium in chloroform at 25°.

---

**Introduction.** – We are carrying out a systematic conformational study with oligopeptides formed by enantiomeric or diastereoisomeric residues (stereo-co-oligopeptides) and having the configurationally different residues in alternating sequence. The two-fold objective [2] of this study is: a better experimental characterization of the conformations of D,L-alternating peptides, and the assessment of the influence that different factors may have on the type of conformation preferred. One of the series is Boc- and MeO-protected oligovalines, and we have reported on the octapeptide Boc-(L-Val-D-Val)<sub>4</sub>-OMe in the crystalline state [3] and in chloroform or cyclohexane [1]. We now present results concerning the dodecapeptide Boc-(L-Val-D-Val)<sub>6</sub>-OMe in the crystalline state by X-ray and IR., and by <sup>1</sup>H-NMR, in CDCl<sub>3</sub> at 25°.

**Results.** – 1. *Boc-(L-Val-D-Val)<sub>6</sub>-OMe in the crystalline state.* – 1.1. *X-ray powder diffraction patterns.* The X-ray powder diffraction patterns of two samples of Boc-(L-Val-D-Val)<sub>6</sub>-OMe, one (12-A) from CHCl<sub>3</sub>/EtOAc and the other (12-B) from CHCl<sub>3</sub>/MeOH, are shown in *Figure 1*, together with the X-ray powder dif-

---

<sup>1)</sup> Part 4 of a series on linear stereo-co-oligopeptides with alternating D- and L-residues. Part 3: [1].

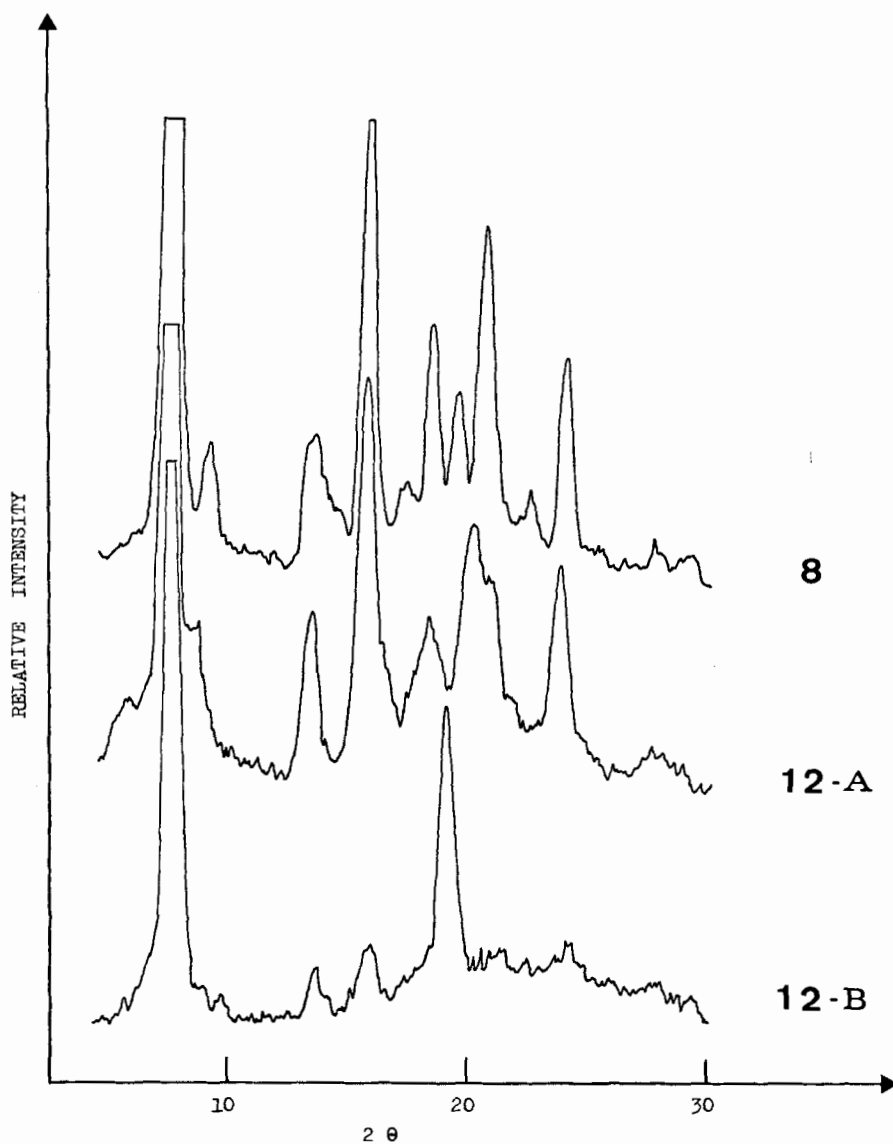


Fig. 1. X-ray powder spectra of Boc-(L-Val-D-Val)<sub>4</sub>-OMe with a  $\beta^{5,6}$  helical structure (8), of Boc-(L-Val-D-Val)<sub>6</sub>-OMe crystallized from CHCl<sub>3</sub>/EtOAc (12-A) and from CHCl<sub>3</sub>/MeOH (12-B)

fraction pattern of a sample of Boc-(L-Val-D-Val)<sub>4</sub>-OMe obtained by recrystallization from EtOAc, and having a  $\beta^{5,6}$  left-handed helical structure [3]<sup>2)</sup>. The pattern of sample 12-A manifests analogies with that of the octapeptide, with regard to both the distribution of the diffracted intensities and the 2θ-values. The X-ray

<sup>2)</sup> For our terminology for the different types of β-helices, see footnote 42 of [1].

pattern of the sample 12-B is different with only two diffraction peaks of relatively high intensity, of which the one at  $2\theta = 19.2^\circ$  is not observable in the pattern of the sample 12-A. The other signals are very weak and probably derive from small amounts of material crystallized with the structure of the sample 12-A.

1.2. *IR. spectra.* The IR. spectra of samples 12-A in Nujol are very similar to the spectrum reported [1] for Boc-(L-Val-D-Val)<sub>4</sub>-OMe in the  $\alpha$   $\beta$ <sup>5,6</sup> left-handed helical structure, with the major amide A, I and II bands at 3300, 1645 and 1538 cm<sup>-1</sup> very similar to those of the octapeptide. Though some variability was observed, IR. spectra of samples 12-B exhibited consistently the amide A and I bands at markedly lower frequencies (3280 and 1638 cm<sup>-1</sup> for one sample, the amide II band being at 1542 cm<sup>-1</sup> in this case) than samples 12-A.

2. *Boc-(L-Val-D-Val)<sub>6</sub>-OMe in CDCl<sub>3</sub>.* – 2.1. *Peculiarities of the <sup>1</sup>H-NMR. spectra.* The <sup>1</sup>H-NMR. spectra of the dodecapeptide in CDCl<sub>3</sub> depended, for a number of hours, on the particular sample and on the time elapsed after the preparation of the solutions. The NH-regions of typical 'initial' spectra (taken immediately after solution) of samples 12-A and 12-B are reproduced in the upper part of *Figure 2* and in *Figure 3*, respectively. Signals of high relative intensity for samples 12-A are of low relative intensity for samples 12-B, and *vice versa*. Similar observations were made for corresponding signals in the other regions of the 'initial' spectra. In time the importance of the signals of very high relative intensity in the 'initial' spectra of samples 12-A decreased markedly but increased in spectra of samples 12-B. 'Final' spectra, whose features remained unchanged at *ca.* 25°, were obtained after 3 to 4 h. *Figure 2* shows the changes that occur in the NH-region of spectra of samples 12-A. The 'final' spectra exhibited the different series of signals prominent in the 'initial' spectra of samples 12-A and of samples 12-B, with relative intensities dependent on the concentration (*Sect.* 2.4), but not on the particular sample.

2.2. *Signal series S(12-A).* In the 'initial' spectra of samples 12-A the signals of high relative intensity (S(12-A)) include a singlet at 1.50 ppm (Boc), a singlet at 3.91 ppm (MeO), and (*Fig. 2*) two doublets (NH) below 7 ppm and ten doublets (NH) between 7.80 and 9.08 ppm. Of the two NH-doublets below 7 ppm, one (6.55 ppm) derives from a Boc-NH-group, since 'initial' spectra of samples 12-A of Boc- $\alpha$ -<sup>2</sup>H-L-Val-(D-Val-L-Val)<sub>5</sub>-D-Val-OMe give an intense singlet at this position, the second was observed between 6.44 and 6.69 ppm in spectra of different solutions.

2.3. *Signal series S(12-B)-1 and S(12-B)-2.* The signals that contribute the most to the 'initial' spectra of samples 12-B – that is, those not belonging to the series S(12-A) – comprise one singlet for Boc-protons (1.48 ppm; another singlet for Boc appears at 1.50, as in the series S(12-A)), two partially overlapping singlets for MeO-protons (3.77 and 3.79 ppm), and two doublets for urethane-NH protons (5.38 and 6.45 ppm). Of these two doublets, assigned on the basis of <sup>1</sup>H-NMR. spectra of Boc- $\alpha$ -<sup>2</sup>H-L-Val-(D-Val-L-Val)<sub>5</sub>-D-Val-OMe and of results of spin-saturation transfer measurements (*Sect.* 2.5), the one located at lower field is generally hidden by overlapping amide-NH signals (*Fig. 3*). In addition 22 amide-NH doublets (by signal integration) contribute to the NH-region. Despite the severe over-

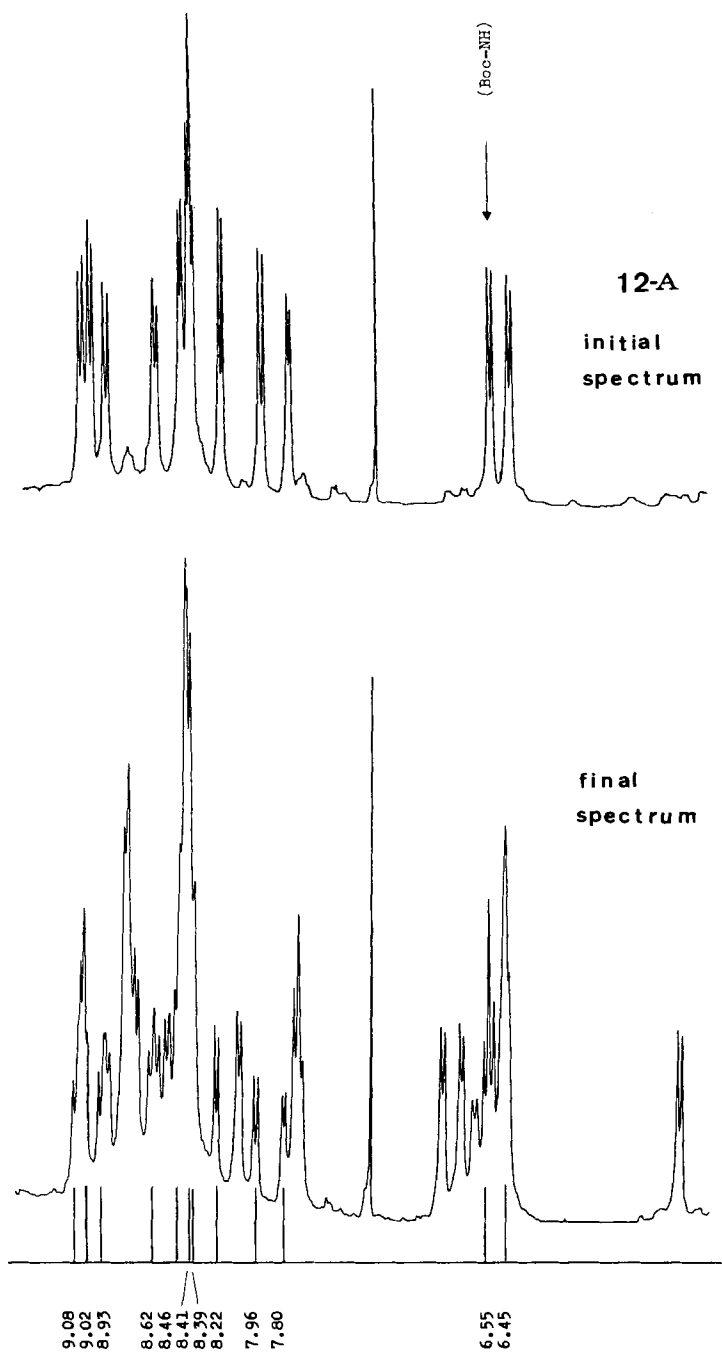


Fig. 2. NH-region of the 'initial' and 'final'  $^1\text{H-NMR}$  spectrum of a sample of  $\text{Boc-(L-Val-D-Val)}_6\text{-OMe}$  crystallized from  $\text{CHCl}_3/\text{EtOAc}$  ( $T$  25°; 19 mg/ml in  $\text{CDCl}_3$ ). The  $\delta$  (ppm) of the 12 NH-doublets of the series S (12-A) are given.

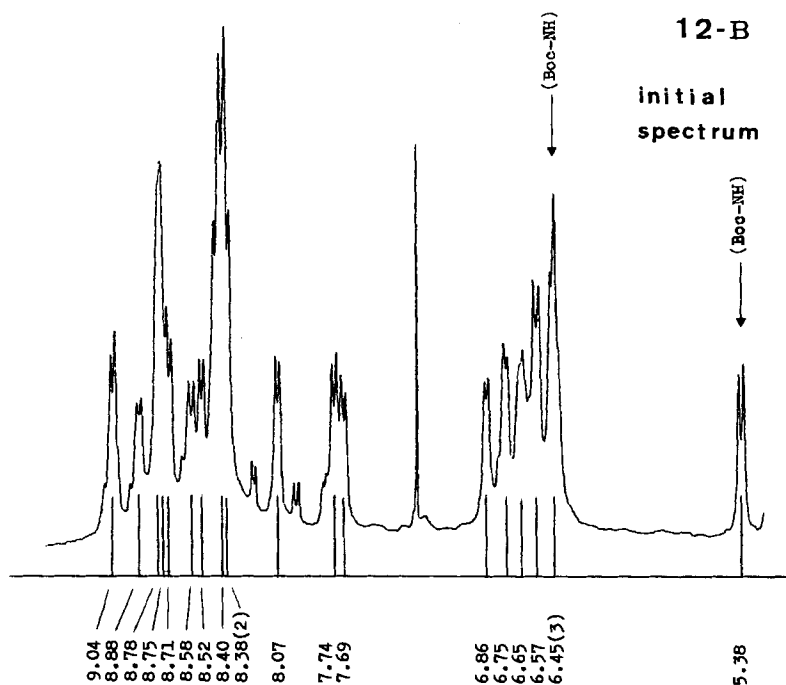


Fig. 3. NH-region of the 'initial' spectrum of a sample of Boc-(L-Val-D-Val)<sub>6</sub>-OMe crystallized from CHCl<sub>3</sub>/MeOH (T 25°; 23 mg/ml in CDCl<sub>3</sub>). The positions of 21 NH-resonance signals of the series S(12-B)-1 and S(12-B)-2 are given.

lapping, we localized 19 of them (Fig. 3) and determined many of the  $^3J(\text{NH}, \alpha\text{-CH})$  with the aid of saturation transfer measurements (Sect. 2.5). The values of  $^3J(\text{NH}, \alpha\text{-CH})$  were all very high (8–10 Hz). Six of the amide-NH resonances are located below 7 ppm with some variation in different spectra. Three of these resonances (6.57, 6.75 and 6.86 ppm in the spectrum of Fig. 3) are slightly more intense (integration) than the other three (two at 6.45 and one at 6.65 ppm in the spectrum of Fig. 3), and the intensities of the signals in the two groups are comparable to those of the Boc-NH resonances at 5.38 and 6.45 ppm. Though overlapping prevented detection of clear differences between the signals of the other types of protons, it is evident that the major signals of the 'initial' spectra of samples 12-B belong to two distinct series of slightly different intensities. We call the series with the more intense signals S(12-B)-1, and that with the less intense signals S(12-B)-2.

2.4. *Relative incidences of the different series.* The relative intensity (ca. 1.2:1) of corresponding signals S(12-B)-1 and S(12-B)-2 seems to be the same in 'initial' and 'final' spectra and does not depend on the particular sample or on concentration. The relative incidence of the series S(12-A) is variable (Sect. 2.1). The ratios of the intensities of the NH-doublets at 7.96 (S(12-A)) and 5.38 ppm (S(12-B)-1) show that the relative incidence of the series S(12-A) in the 'final' spectra tends to

Table. Representative values of the ratio *R* between the intensities of the amide-NH signal at 7.96 ppm of the series S(12-A) and of the urethane-NH signal at 5.38 ppm of the series S(12-B)-1

Sample	Conc. (g/ml)	<i>R</i>	
		'Initial' spectrum	'Final' spectrum
12-B	0.030	0.2	0.5
a)	0.021	0.9	0.5
12-A	0.019	15	0.4
12-B	0.018	0.3	0.4
12-A	0.007	b)	0.2

a) Sample obtained by evaporation of a solution of the dodecapeptide in CHCl<sub>3</sub>. b) Not determined.

decrease with increasing dilution, while that of the series S(12-B)-1 - and S(12-B)-2 - increases (Table).

2.5. *Spin-saturation transfer.* The NH-signals below 7 ppm of a 'final' spectrum (top left corner of Fig. 4) were selectively irradiated, and the transfer of saturation was observed in the difference spectra *a-e*. Under the conditions employed no transfer of saturation to or from signals S(12-A) was observed: for instance, no doublet at 6.55 ppm, that would derive from the transfer to the Boc-NH-signal S(12-A) of the saturation of the Boc-NH-signal S(12-B)-1 was detected in the difference spectrum *a*. Thus, the effects observed (Fig. 4) are ascribable only to signals S(12-B)-1 and S(12-B)-2. The difference spectra *b-e* show that saturation of the amide-NH signals of these two series located below 7 ppm is always and exclusively transferred to signals located at much lower field. The amide-NH signal at 6.63 ppm was not irradiated directly; however, the effect produced by the direct irradiation of either of the two adjacent signals indicates that it has a saturation transfer to a signal at 8.40 ppm (see dashed arrow in the difference spectrum *d*). Such saturation transfer measurements allowed us to identify the positions, and determine the <sup>3</sup>*J*(NH, *α*-CH) of several NH-doublets S(12-B)-1 and S(12-B)-2, that overlap in spectra with no saturation.

**Discussion.** - The analogies found in the X-ray powder-diffraction patterns and in the IR. spectra for Nujol mulls show that the crystal structure of samples 12-A of Boc-(L-Val-D-Val)<sub>6</sub>-OMe is predominantly a double-stranded  $\beta$ -helical structure of the type  $\pi$   $\beta^{5,6}$ , with left-handed sense of twist, like that of Boc-(L-Val-D-Val)<sub>4</sub>-OMe [3]. The data available so far do not allow any conclusion regarding the type of crystal structure for samples 12-B of the dodecapeptide. The position at 3280 cm<sup>-1</sup> of the amide A band of these samples hints at stronger H-bonds than those formed by samples 12-A in the double helix.

The <sup>1</sup>H-NMR. results in CDCl<sub>3</sub> indicate three different conformational species for Boc-(L-Val-D-Val)<sub>6</sub>-OMe, interconverting slowly enough to give rise to separate series of signals in the <sup>1</sup>H-NMR. spectra. Particularly low is the rate of formation and conversion of the species associated with the series S(12-A), and at 25° some hours are needed to reach conformational equilibrium. The interconversion between the two species associated with S(12-B)-1 and S(12-B)-2 is a much more rapid process, which can be observed by spin saturation transfer experiments (Sect. 2.5). In view of its very low conversion rate, the structure of the species predominating

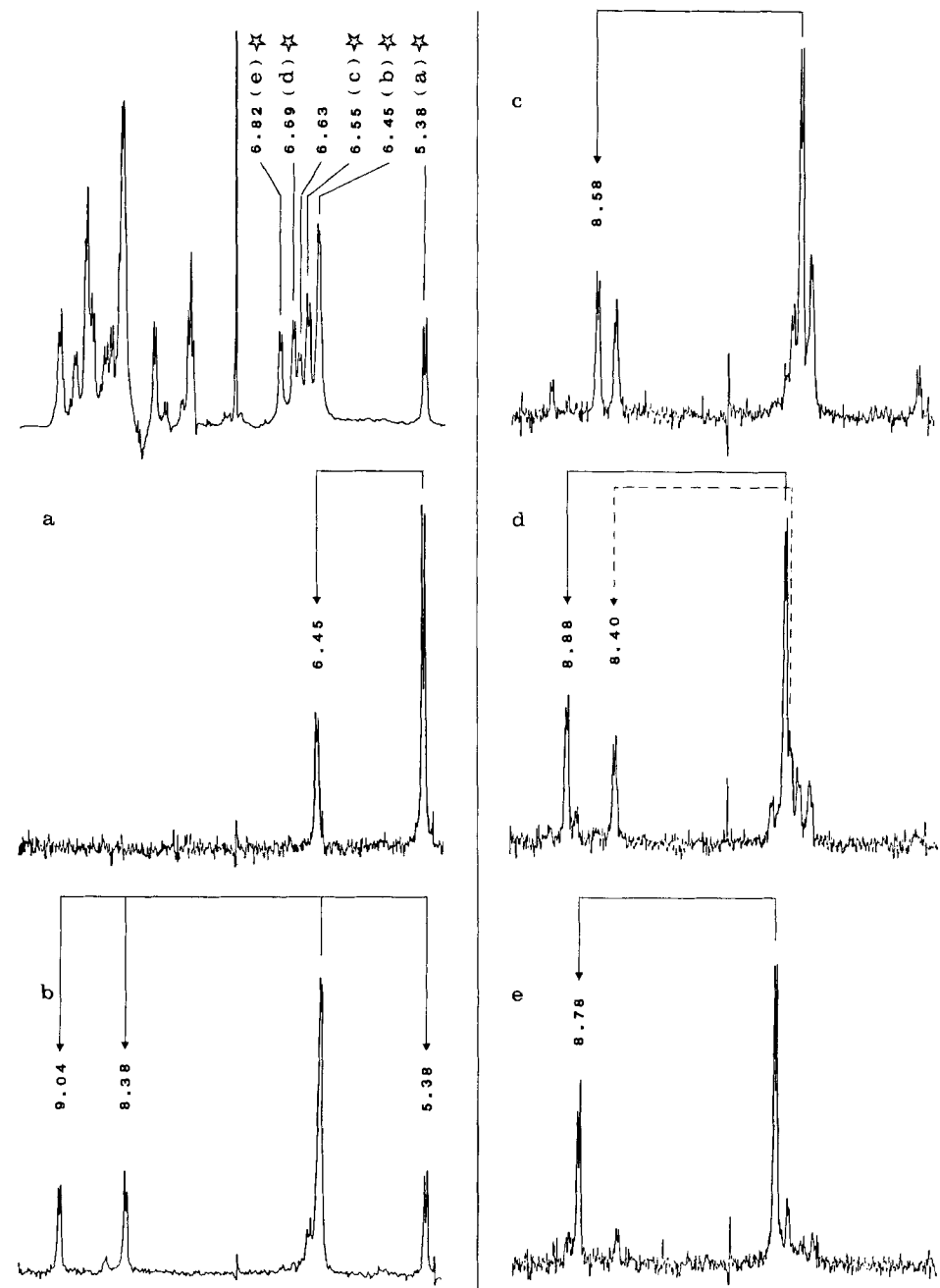


Fig. 4. Transfer of the saturation of the NH-resonance signals below 7 ppm in the 'final' spectrum of *Boc-(L-Val-D-Val)<sub>6</sub>-OMe* (T 25°; 7 mg/ml in CDCl<sub>3</sub>). Selectively irradiated signals are indicated by a star in the spectrum with no saturation (top left), and the corresponding transfers are indicated by arrows in the difference spectra a-e. The dashed arrow in the difference spectrum d indicates the transfer of saturation for the signal at 6.63 ppm, which has not been irradiated directly (see text).

in freshly prepared solutions of samples 12-A may be similar to that of the samples in the crystalline state. The following considerations indicate that this is the case. The characteristics of the series S(12-A) (*Sect.* 2.2) are very similar to those of the signals characterizing [1] the  $^1\text{H-NMR}$ . spectrum of the left-handed,  $\pi\beta^{5.6}$  helical species of Boc-(L-Val-D-Val)<sub>4</sub>-OMe in  $\text{CDCl}_3$ . In particular, signals of the Boc- and MeO-groups, and of the urethane-NH have the same position, and both series have only one amide-NH doublet at slightly variable positions below 7 ppm. Therefore the species associated with the series S(12-A) also has a double-stranded, left-handed, helical structure of the type  $\pi\beta^{5.6}$ . For this species ten amide-NH groups per chain are expected to be involved in interstrand H-bonding, and ten amide-NH doublets are observed at low field between 7.80 and 9.08 ppm for the series S(12-A) (*Fig.* 2).

With the assignment of the series S(12-A) to a dimeric species, the type of concentration dependence observed for the relative incidences of the different series in the 'final' spectra (*Table*) seems to indicate that the two species associated with the series S(12-B)-1 and S(12-B)-2 are monomeric. The high values of the vicinal coupling constants  $^3J(\text{NH}, \alpha\text{-CH})$  strongly suggest that they are  $\beta$ -helices. The H-bonding pattern schemes of *Figure 5* show that the dodecapeptide in a right-handed  $\beta^{4.4}$  helix would have a non-H-bonded urethane-NH and three non-H-bonded amide-NH, and in a left-handed  $\beta^{4.4}$  helix a H-bonded urethane-NH and three non-H-bonded amide-NH. These situations can be deduced from the positions of the NH-signals for the species associated with the series S(12-B)-1 and S(12-B)-2 (*Sect.* 2.3). The relationship between position of the signals of NH-groups and H-bonded or non-H-bonded state of these groups [1] indicates that the Boc-NH-signals of S(12-B)-1 at 5.38 ppm, and of S(12-B)-2 at 6.45 ppm, derive from a non-H-bonded and a H-bonded group, respectively, and that the three amide-NH resonances below 7 ppm of each series derive from non-H-bonded NH-groups. This concurs with the observed variation of the position of these amide-NH resonances (*Sect.* 2.3), which possibly reflects an interaction of the free NH-groups with traces of water in  $\text{CDCl}_3$ . Thus, the species associated with S(12-B)-1 appears to be a right-handed  $\beta^{4.4}$  helix, and the species associated with S(12-B)-2 a left-handed  $\beta^{4.4}$  helix. This conclusion is strengthened by the results of the spin-saturation transfer measurements (*Sect.* 2.5). *Figure 5* shows that the amide-NH that are free in one helix are bonded in the other, and we indeed observed (*Fig.* 4) transfer of the saturation of signals of the free amide-NH groups (below 7 ppm) to signals of bonded amide-NH groups (above 7 ppm).

These conformational assignments provide a rationale for the different rates of species interconversion observed. These rates probably depend on the number of H-bonds that must be opened and reformed during the interconversion process. The double helix has 22 H-bonds; the single-stranded helices only eight (right-handed) or nine (left-handed). It is therefore not surprising that the interconversion processes involving the double helix are by far the slowest.

**Conclusion.** – Boc-(L-Val-D-Val)<sub>6</sub>-OMe forms three species in  $\text{CHCl}_3$ . One of them is dimeric with a left-handed helical structure of the type  $\pi\beta^{5.6}$  similar to the crystal structure of dodecapeptide crystallized from  $\text{CHCl}_3/\text{EtOAc}$ . The other two



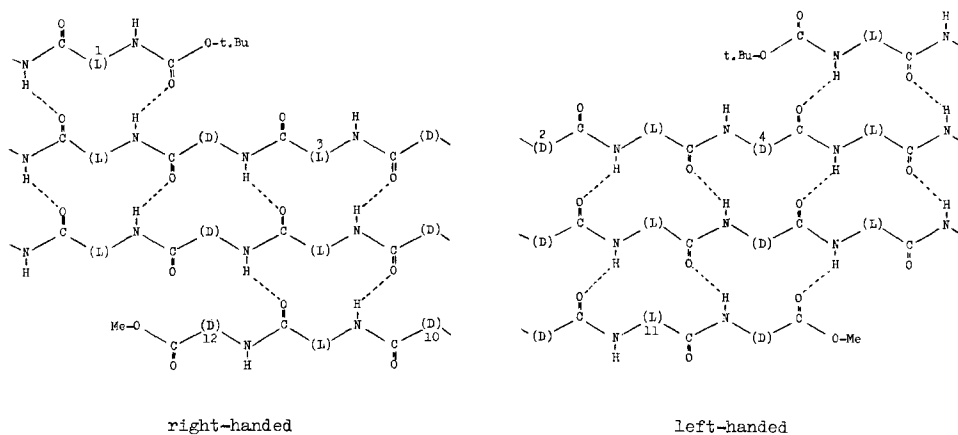


Fig. 5. H-bonding pattern of the two  $\beta^{4.4}$  helical structures of Boc-(L-Val-D-Val)<sub>6</sub>-OMe of opposite handedness. The diagrams look at helices split along the back and laid out flat. The sequence numbers of the residues in which the NH is free are indicated.

species are monomeric, and likely a right-handed and a left-handed  $\beta^{4.4}$  helix. The three species interconvert slowly enough in  $\text{CHCl}_3$  to give separate  $^1\text{H-NMR}$  signals. The processes are schematically summarized in Figure 6. At the moment it is not known whether the double helix converts into or is formed from only one or both of the single helices, and the bracket in Figure 6 reflects this uncertainty.

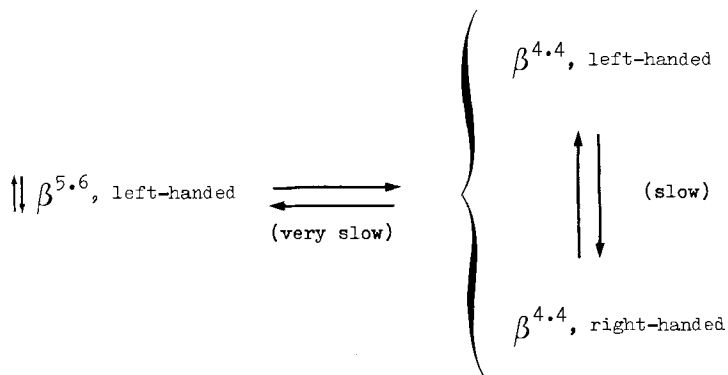


Fig. 6. Interconversion of the  $\beta$ -helical species of Boc-(L-Val-D-Val)<sub>6</sub>-OMe in  $\text{CHCl}_3$

The system formed by the dodecapeptide in  $\text{CHCl}_3$  is very attractive for a kinetic study of the mechanism of interconversion of  $\beta$ -helices of different type, and we plan to start this study.

Partial financial support for this investigation by the Swiss National Science Foundation is gratefully acknowledged. Help with the manuscript from B. Straub is deeply appreciated.

### Experimental Part

**Materials.** Boc-(L-Val-D-Val)<sub>6</sub>-OMe was prepared and purified as described [2]. Boc-*a*-<sup>2</sup>H-L-Val-(D-Val-L-Val)<sub>5</sub>-D-Val-OMe with about 85% deuteration at the *a*-C-position of the N-terminal residue was synthesized from Boc-*a*-<sup>2</sup>H-L-Val-(D-Val-L-Val)<sub>3</sub>-D-Val-OMe [4]. The octapeptide was hydrolyzed to the corresponding Boc-octapeptide acid, which was condensed with H-(L-Val-D-Val)<sub>2</sub>-OMe (cf. [2]). Samples of the dodecapeptide used were obtained by slow evaporation in air of solutions in CHCl<sub>3</sub>/EtOAc (12-A) or by evaporation in a rotary evaporator of solutions in CHCl<sub>3</sub>/MeOH (or MeOH) (12-B) then drying in high vacuum at 85°.

**Methods.** X-ray powder-diffraction patterns were recorded with a *Phillips PW 100* X-ray diffractometer using CuK $\alpha$ -radiation ( $\lambda = 1.5418 \text{ \AA}$ ). IR. spectra were determined with a *Perkin-Elmer 177* spectrophotometer (solids in Nujol). The position of the bands are accurate to  $\pm 5 \text{ cm}^{-1}$  in the amide A region and to  $\pm 2 \text{ cm}^{-1}$  in the amide I and II region. <sup>1</sup>H-NMR. spectra were carried out with a *Bruker HXS-360* spectrometer at 25° in CDCl<sub>3</sub> with TMS as internal standard. Spin-saturation transfer difference spectra were obtained by using the same pulse sequence as used [5] for measuring driven nuclear *Overhauser* effects. The irradiation time was 0.5 s. The solutions of the dodecapeptide were prepared and kept at r.t. (22–25°). Because of the limited solubility of the samples solutions with concentration of 7–30 mg/ml were used.

### REFERENCES

- [1] G.P. Lorenzi, H. Jäckle, L. Tomasic, V. Rizzo & C. Pedone, *J. Am. Chem. Soc.* **104**, 1728 (1982).
- [2] L. Tomasic, A. Stefani & G.P. Lorenzi, *Helv. Chim. Acta* **63**, 2000 (1980).
- [3] E. Benedetti, B. Di Blasio, C. Pedone, G.P. Lorenzi, L. Tomasic & V. Gramlich, *Nature* **282**, 630 (1979).
- [4] G.P. Lorenzi, H. Jäckle & L. Tomasic, in preparation.
- [5] A. Dubs, G. Wagner & K. Wüthrich, *Biochim. Biophys. Acta* **577**, 177 (1979).